Virology 588 (2023) 109910

Contents lists available at ScienceDirect

Virology

journal homepage: www.elsevier.com/locate/virology

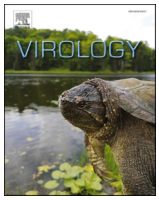

A new member of the *Nudiviridae* from the Florida stone crab (*Menippe mercenaria*)

Jamie Bojko [a,b,*], Elizabeth Duermit-Moreau [c], Ryan Gandy [d], Donald C. Behringer [c,e]

[a] National Horizons Centre, Teesside University, Darlington, DL1 1HG, United Kingdom
[b] Teesside University, Middlesbrough, TS1 3BX, United Kingdom
[c] Fisheries and Aquatic Sciences, University of Florida, Gainesville, FL, 32653, USA
[d] Florida Fish and Wildlife Research Institute, St. Petersburg, FL, 33701, USA
[e] Emerging Pathogens Institute, University of Florida, Gainesville, FL, 32611, USA

ARTICLE INFO

Handling Editor: Dr. Jasmine Tomar

Keywords:
Virus
Virology
Fishery
Brachyura
Ecology
Disease
Crustacea

ABSTRACT

Menippe mercenaria, the Florida stone crab, supports an unconventional fishery across the southern USA and Caribbean that involves claw-removal and the return of de-clawed animals to the sea. We provide pathological, ultrastructural, and genomic detail for a novel hepatopancreatic, nucleus-specific virus - Menippe mercenaria nudivirus (MmNV) - isolated from *M. mercenaria*, captured during fisheries-independent monitoring.

The virus has a genome of 99,336 bp and encodes 84 predicted protein coding genes and shows greatest similarity to Aratus pisonii nudivirus (ApNV) (<60% protein similarity and 31 shared genes of greatest similarity), collected from the Florida Keys, USA. MmNV is a member of the *Gammanudivirus* genus (*Naldaviricetes*: *Lefavirales*: *Nudiviridae*). Comparisons of virus genome size, preferred host environment, and gene number revealed no clear associations between the viral traits and phylogenetic position. Evolution of the virus alongside the diversification of host taxa, with the potential for host-switching, remain more likely evolutionary pathways.

1. Introduction

The Florida stone crab (*Menippe mercenaria*) is a brachyuran species fished in the south-eastern United States and several Caribbean nations, with ~99% of landings occurring in Florida, USA. The fishery practices claw removal, wherein fishers attempt to remove legal-sized claws along the natural fracture plane for autotomy, and the live crabs are returned to the water. Crabs can survive this practice and regenerate lost claws; however, studies suggest that claws are often not broken at the natural fracture plane and survival is just 20–40% for crabs with two claws removed (Duermit et al., 2015; Gandy et al., 2016) and only 4–13% survive to regenerate claws and re-enter the fishery (Muller et al., 2006; Duermit et al., 2017). Due to the injury suffered and the increased energetic demand of claw regeneration, perhaps including reduced prey access, de-clawed individuals may be more prone to acquiring disease (Duermit et al., 2015; Hancock and Griffen, 2017). Fishing can alter the prevalence of parasitism, often causing decreases in directly transmitted diseases due to related decreases in host density (Wood et al., 2014). However, any reduction in host density due to fishing may be offset by the use of traps to capture *M. mercenaria*. Traps unnaturally concentrate individuals, facilitating transmission, then potentially infected sublegal crabs and those from which claws have been harvested are released back into the population (Freeman and MacDiarmid, 2009; Behringer et al. 2012, 2020). These divergent scenarios highlight the need to better understand *M. mercenaria* pathologies and associated disease ecology.

Little is known about the diseases of *M. mercenaria*, aside from a handful of associations, including: the dinoflagellate *Hematodinium perezi* (Sheppard et al., 2003); apicomplexan gregarines (Duermit-Moreau et al., 2022), *Nematopsis ostrearum* (Sprague and Orr, 1955) and *Nematopsis prytherchi* (Sprague, 1949); the stalked gill barnacle, *Octolasmis mulleri* (Humes, 1941); and the nemertean egg predator *Carcinonemertes caissarum imminuta* (Santos et al., 2006). Viral pathogens of this crab species have yet to be described.

A common pathogen group in decapod crustaceans are members of the *Nudiviridae*, a family of dsDNA viruses that target the nuclei of the crustacean host's hepatoancreatocytes. The recent burst in discovering members of this viral family has led to concern about their pathological role in beneficial invertebrates (Yang et al., 2014; Holt et al., 2019; Allain et al., 2020; Bateman et al., 2021; Bojko et al. 2022a, 2022b); however, we know little about their effect on fished populations. Here,

* Corresponding author. National Horizons Centre, Teesside University, Darlington, DL1 1HG, United Kingdom.
E-mail address: J.Bojko@tees.ac.uk (J. Bojko).

https://doi.org/10.1016/j.virol.2023.109910
Received 16 August 2023; Received in revised form 4 October 2023; Accepted 9 October 2023
Available online 10 October 2023

we present the first viral pathogen of *M. mercenaria*, a nudivirus (dsDNA; *Nudiviridae*) isolated from the hepatopancreas of the Florida stone crab. We provide histopathological, ultrastructural, and genomic detail for the newly isolated 'Menippe mercenaria nudivirus' (MmNV) and explore genomic relatedness and environmental parameters between this new nudivirus and previously discovered nudiviruses form arthropod hosts.

2. Materials and methods

2.1. Sample collection, tissue preservation, and histological processing

Menippe mercenaria were collected offshore from Cedar Key, Florida, USA in October 2019 (n = 53), December 2019 (n = 50), and June 2020 (n = 52) alongside Florida Fish and Wildlife Conservation Commission's (FWC) Fish and Wildlife Research Institute Crustacean Research Project (FWRI-CRP). Four lines of five traps were baited with pig feet, deployed, and soaked for 12–16 d. Plastic commercial stone crab traps (40.6 cm × 40.0 cm x 30.5 cm) with a vertically mounted entrance funnel (14.0 cm × 8.9 cm) and an escape opening (14.0 cm × 8.9 cm), covered with a degradable pine slat, were used. All trapped crabs above 55 mm carapace width (CW) were collected, except for ovigerous females. Crabs were placed in cooled, oxygenated seawater until necropsy. Stone crabs were euthanized and necropsied within 24 h of capture at the Aquatic Pathology Laboratory (APL) at the University of Florida in Gainesville, Florida.

During necropsy, muscle, hepatopancreas, gonad, gill, heart, midgut, antennal gland, and epithelial tissues were biopsied and fixed in Davidson's saltwater fixative (formaldehyde, acetic acid, glycerol, ethanol, seawater). Tissues were soaked for 24–48 h and then transferred to 70% ethanol until they were processed by the FWC-FWRI Histology Department. The tissues were wax infiltrated, embedded, sectioned at a thickness of 4 μm, and mounted on glass slides. Slides were then rehydrated and stained with haematoxylin and alcoholic eosin (H&E). The slides were screened for viral-like pathologies using a standard light microscope with an integrated Leica camera.

2.2. Transmission electron microscopy

Infected hepatopancreatic tissue was preserved in 2.5% glutaraldehyde in 0.1% sodium cacodylate buffer. Tissue was dissected into smaller 1 mm^3 sections and warmed using a Pelco BioWave Pro laboratory microwave (Ted Pella, Redding, CA, USA). Samples were washed in 0.1 M sodium cacodylate (pH 7.24) and post-fixed with buffered 2% OsO_4, rinsed with water and the dehydrated in an ethanol series (25%–100%, 5–10% increments) followed by 100% acetone. Dehydrated samples were then infiltrated with ARALDITE/Embed (Electron Microscopy Sciences (EMS), Hatfield, PA) and embedding primer (Z6040; EMS, Hatfield, PA) in increments of 3:1, 1:1, 1:3 anhydrous acetone: ARALDITE/Embed, followed by 100% ARALDITE/Embed resin. Semithin sections (500 nm) were then stained with toluidine blue and viewed under a Leica light microscope to identify infected nuclei. Following trimming of the block, ultra-thin sections (50–80 nm) were collected on nickel-coated Formvar 100 mesh grid (EMS, Hatfield, PA) and treated with 1% sodium periodate (meta) (Fisher Scientific, Fair Lawn, NJ). The grid(s) were post-stained with 2% aqueous uranyl acetate [$UO_2(CH_3COO)_2$] and lead citrate ($C_{12}H_{10}O_{14}Pb_3$) (EMS, Hatfield, PA). The sections were examined with an FEI Tecnai G2 Spirit Twin TEM (FEI Corp., Hillsboro, OR) and digital images were taken using a Gatan UltraScan 2k × 2k camera, equipped with Digital Micrograph software (Gatan Inc., Pleasanton, CA). Viral measurements were acquired from the resulting images using ImageJ. The above methods closely follow the processes described in Stratton et al. (2023a, 2023b).

2.3. DNA extraction, library preparation and metagenomic sequencing

DNA was extracted from the hepatopancreatic tissue of one animal exhibiting hypertrophic epithelial nuclei at APL using a Qiagen DNeasy blood and tissue extraction kit according to the manufacturer's protocols. The DNA extract was shipped to Novogene Corporation for metagenomic sequencing. The DNA (1 μg) was used to prepare a NEBNext® Ultra™ DNA Library (Illumina) following manufacturer's instructions. The library was paired-end sequenced on an Illumina NovaSeq 6000 with the 150 bp NovaSeq 6000 SP reagent kit (300 cycles). The run produced 2.84 x 10^6 forward and 3.05 x 10^6 reverse raw reads, which were trimmed using Trimmomatic v0.39 (specifications: LEADING: 3 TRAILING: 3 SLIDINGWINDOW: 4:15 MINLEN: 36) (Bolger et al., 2014). Assembly of the trimmed reads (paired and unpaired) was conducted using SPAdes v3.15.3 (Bankevich et al., 2012) and the assembly statistics determined using Quast v5.0.2 (N50: 1260; N75: 877; L50: 136,207; L75: 262,806) (Gurevich et al., 2013). The assembly resulted in 212,358 contiguous nucleotide sequences above 1000bp. The contigs were screened for similarity using a bespoke NCBI database based on all available proteins from members of the *Nudiviridae*, using blastx, resulting in four contigs that resembled a nudivirus genome. The four contigs were individually mapped and aligned, resulting in a contiguous circular sequence (99,336bp, 70X coverage) that was identified as a putative nudivirus genome. The genome was subject to mapping to confirm continuity with the help of CLC genomics workbench v.12.

2.4. Viral genome annotation and genomic comparisons

The nudivirus genome was re-oriented to start at the predicted DNA polymerase and annotated using GeneMarkS (Besemer et al., 2001) as well as manually searched for smaller coding regions that encoded the p6.9 gene (ExPASy translate; Gasteiger et al., 2003). Seventeen of the core proteins (*DNApol, helicase, lef-4, lef-5, lef-8, lef-9, p74, vp39, vp91, 38k, ac81, pif-1, pif-2, pif-3, pif-4, pif-5, pif-6*), shared by all known members of the *Nudiviridae*, were aligned using MAFFT and concatenated manually to produce a single alignment file. The file consisted of 14,681 columns, 10,500 distinct patterns (7401 parsimony-informative), 2758 singleton sites, and 4522 constant sites and was then used in conjunction with IQ-Tree v2.1.3 (multicore CoVID-edition for Linux 64-bit) to produce a maximum-likelihood phylogenetic tree (1000 bootstrap) based on the evolutionary model: Q.pfam + F + I + G4, according to Bayesian Information Criterion (Nguyen et al., 2015). The log likelihood of the final tree was −274, 596.127 for the 15 nudiviruses involved.

2.5. Graphical plots

Information pertaining to the genome size, number of encoded and predicted protein coding genes, host habitat, and viral taxonomy for all nudiviruses identified to date were tabulated and analysed in R v.4.0.3 and RStudio (R Core Team, 2013). The package ggplot2 (Wickham, 2011) was used to plot the data. In addition, the package gggenes (cran.r-project.org/web/packages/gggenes/) was used to plot the coding regions of several *Gammanudivirus* members, including the new isolate. The circular genome architecture was visualised in Circa (omgenomics.com/circa/).

3. Results

3.1. Hepatopancreatic pathology, viral prevalence, and ultrastructure

Histological slides of the hepatopancreas for 155 specimens *M. mercenaria* included a virus-like pathology in 26 individuals across all three collection periods [October 2019 (n = 9), December 2019 (n = 7), June 2020 (n = 10)], consisting of a hypertrophic, basophilic-staining nuclei of one or more hepatopancreatic epithelial cells (Fig. 1). Similar hypertrophic nuclei were not observed in other tissue types. The hepatopancreatic tubules of infected individuals did not appear to be

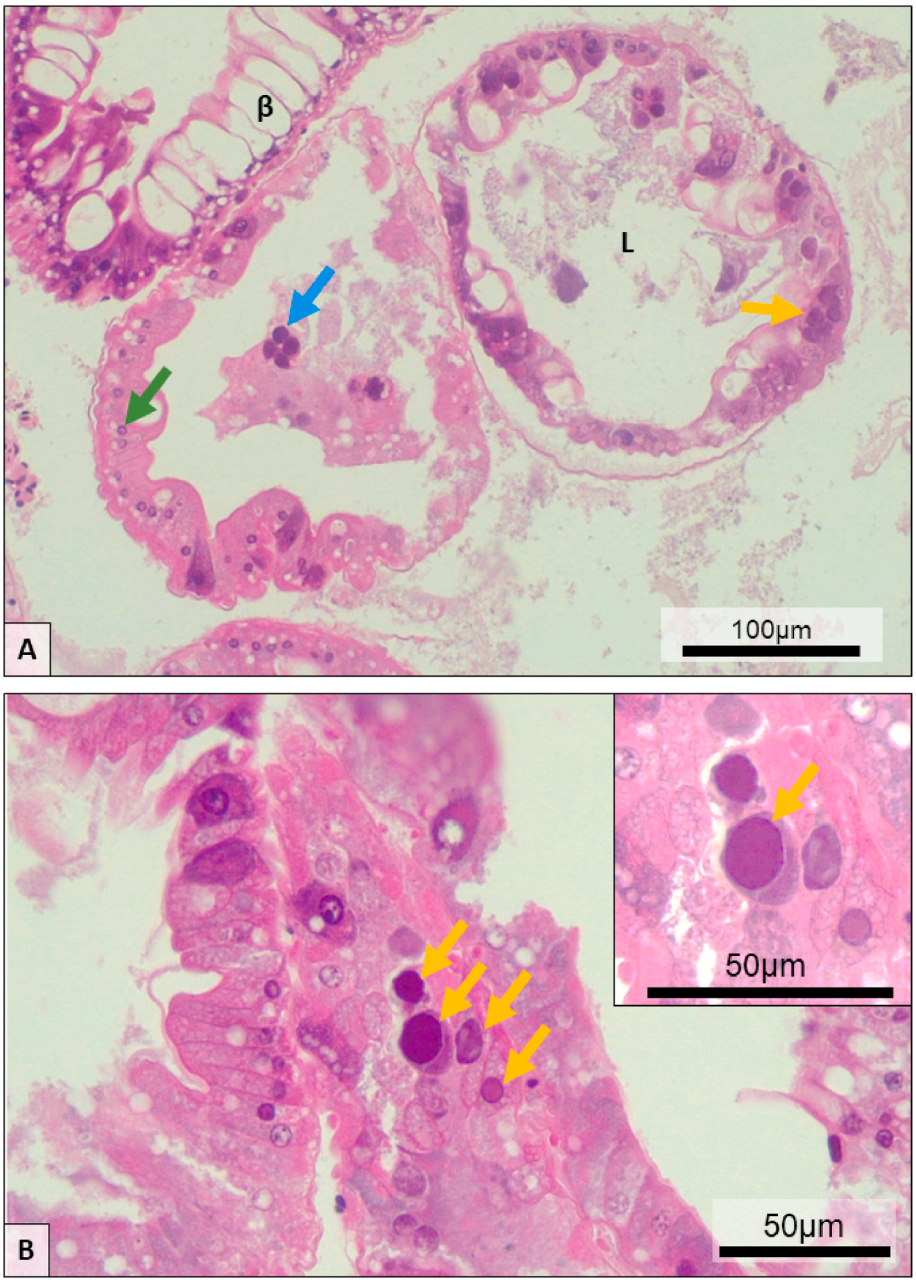

Fig. 1. Hepatopancreatic pathology of a nudivirus-infected individual. A) A X20 image of three hepatopancreatic tubules (including β-cells, indicated on the figure) at different stages of deterioration. The orange arrow indicates an uninfected nucleus. The blue arrow indicates several infected nuclei in cells sloughing into the lumen. The yellow arrow indicated infected nuclei in cells still attached to the basement membrane. B) A X40 image of several infected nuclei that appear as different stages of infection. The inset image identified a hypertrophied nucleus with the growing viroplasm inside, which stains basophilic and exhibiting marginated chromatin.

degraded in any way and the basement membrane and epithelial layer appeared intact; however, in some individuals there were examples of infected cells sloughing off into the hepatopancreatic lumen. The basophilic-staining inclusion of the affected nuclei appeared to be a putative viroplasm, forcing the host chromatin to appear at the margin of the nuclear membrane, visible as a deep-blue staining ring. No obvious gross clinical signs or behavioural differences were noted for the 26/155 (16.8%) infected individuals and the viral pathology was only observable under histological section.

Transmission electron micrographs of infected nuclei revealed a membrane-bound bacilliform-shaped virus with a crooked appearance of the genomic core and slight expansion of the anterior membrane (Fig. 2). The core of each virion was 0.172 ± 0.034 μm in length and 0.022 ± 0.004 μm in width (SD, n = 12). The total length, including the membrane, was 0.215 ± 0.033 μm and the width was 0.059 ± 0.011 μm (SD, n = 12).

3.2. *Nudivirus genome architecture, comparative genomics, and phylogenetics*

The genome of MmNV consists of a 99,336 bp circular dsDNA molecule and encoded 84 predicted protein coding genes (NCBI accession: OQ725696; Fig. 3). All core nudivirus genes are encoded on the MmNV genome, including the duplicated *helicase 2* and *vlf-1* genes common among *Gammanudivirus* members (Fig. 4). MmNV encodes only one *odv-e66*, similar to 'Aratus pisonii nudivirus' (ApNV) and Carcinus

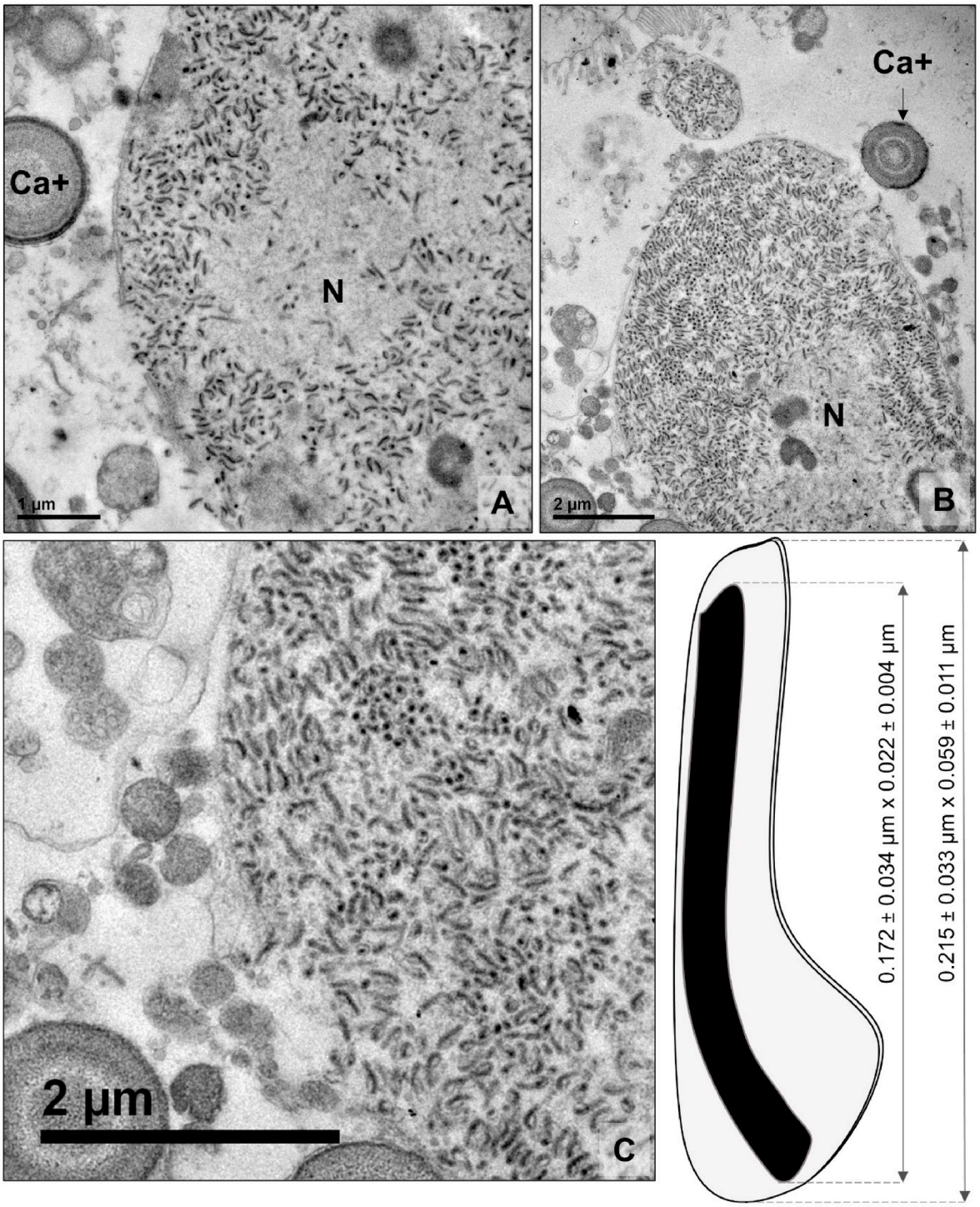

Fig. 2. Transmission electron micrographs of nudivirus-infected hepatopancreatocytes. A-B) Transmission electron micrographs of two infected nuclei (N) displaying bacilliform virions in hepatopancreatic epithelial cells, accompanied by large calcium crystals (Ca+). Darker areas within the centre of the infected nuclei are thought to be viral factories. An accompanying vesicle transporting virus out of the cell is present in image B. C) A higher magnification image shows the virions in more detail, including their electron dense genome, slight crooked appearance, and their membrane. A cartoon of the virus is present along with measurement information.

maenas nudivirus (CmNV; from the species *Gammanudivirus cameanadis*); however, the position of this gene is the same between MmNV and ApNV, whereas it appears to have been translocated in CmNV (Fig. 4). Genome synteny is most similar between MmNV and ApNV, relative to other nudiviruses; however, the synteny is broken by an apparent insertion of genes ApNV_40 – ApNV_43 in the ApNV genome, which are missing from the MmNV genome. Genes ApNV_40 – ApNV_42 encoded hypothetical proteins with no known function, but the ApNV_43 gene encoded a protein with some similarity to proteins from *Chionoecetes opilio* and other crustacean proteins, but with a low e-value (KAG0713444; similarity: 35%; coverage: 70%; e-value: $8e^{-25}$). Coverage of the MmNV genome strongly supports that this series of proteins are part of the genome and unlikely to have been incorrectly incorporated during assembly (Fig. 3). A single gene appears to be in place of this region in the MmNV genome, which encodes a hypothetical protein with no currently predictable function.

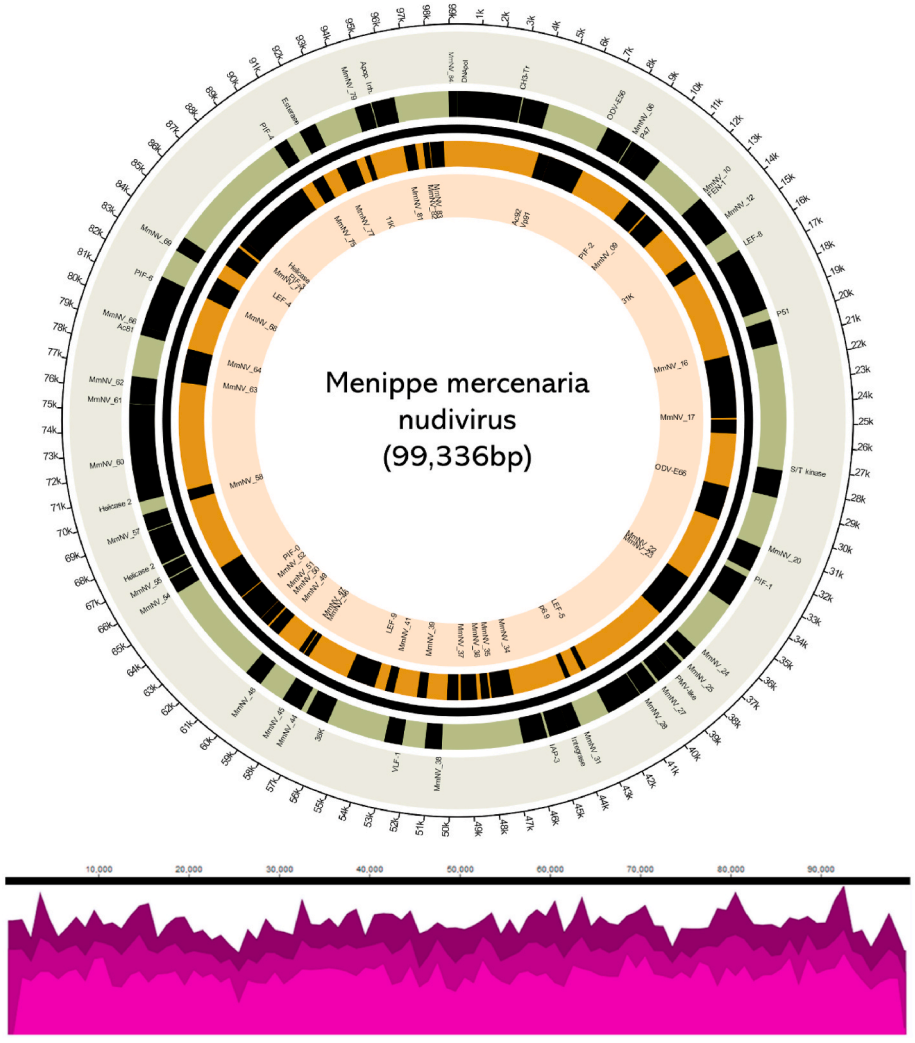

Fig. 3. A circular plot of the genome architecture of Menippe mercenaria nudivirus (MmNV). The genome is 99,336 bp in length and encodes 84 predicted protein coding genes (GeneMarkS). Positive strand coding genes are presented above the genome line with a green background. The negative strand coding genes are encoded beneath the genome line with an orange background. The names of the individual genes/proteins are listed at the start codon of each gene. Beneath the circular plot is a mapping plot of individual trimmed reads across the genome, highlighting the coverage (y axis minimum 0 – y axis maximum 242, times coverage) across the genome (light to dark colour indicates forward, reverse, and overall coverage).

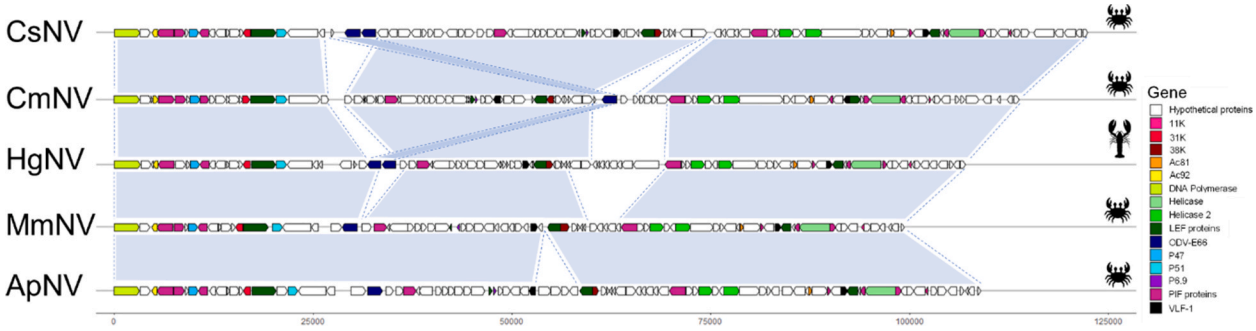

Fig. 4. Genome architecture plots for five of the most similar *Gammanudivirus* members, including: 'Callinectes sapidus nudivirus' (CsNV); Carcinus maenas nudivirus (CmNV); Homarus Gammarus nudivirus (HgNV); 'Menippe mercenaria nudivirus' (MmNV); and 'Aratus pisonii nudivirus' (ApNV). Regions of similarity (excluding small changes, such as gene orientation) are highlighted in light blue, and overlapping blue polygons refer to changes in gene synteny between the viruses. A lack of blue shading suggests a larger change in coding gene presence or synteny.

Protein similarity between MmNV and ApNV is most common (31 proteins), with fewer proteins similar to other gammanudiviruses (CmNV: 14; CsNV: 12; HgNV: 7; MrNV: 2; PmNV: 1) (Table 1). Fifteen predicted proteins did not show any similarity to other proteins (Table 1). The most similar protein to another nudivirus was the ODV-E66 protein (coding gene: MmNV_19), which was 67.7% similar to the ODV-E66 protein encoded by 'Callinectes sapidus nudivirus' (CsNV; Bojko et al., 2022b).

Table 1
Menippe mercenaria nudivirus protein sequence similarity table, comparing the predicted proteins from 84 hypothetical protein coding genes to those of other nudiviruses. The most similar protein hit is listed in the table.

Gene	Start	Stop	Protein hit (species; accession)	Similarity (%)	e-value
MmNV_01	1	3135	DNA polymerase (CmNV; UBZ25591)	49.7	0.0
MmNV_02	3187	4461	Methyltransferase (ApNV; UOT91767)	35.3	1.0e-71
MmNV_03	4672	5352	Ac92-like protein (CmNV; UBZ25594)	48.8	8.7e-67
MmNV_04	5349	7370	Vp91 (ApNV; UOT91769)	44.1	0.0
MmNV_05	7498	8805	ODV-E56 (ApNV; UOT91770)	61.0	4.4e-164
MmNV_06	8851	9288	Hypothetical (CmNV; UBZ25597)	39.0	6.5e-24
MmNV_07	9285	10487	P47 (CsNV; UVX94867)	41.3	4.0e-107
MmNV_08	10484	11662	PIF-2 (ApNV; UOT91773)	61.4	2.7e-164
MmNV_09	11767	13047	Hypothetical (CmNV; UBZ25601)	26.3	4.0e-22
MmNV_10	13128	13463	Hypothetical (ApNV; UOT91776)	28.6	2.9e-13
MmNV_11	13436	14698	FEN-1 (ApNV; UOT91777)	35.9	3.6e-86
MmNV_12	14691	15176	Hypothetical (ApNV; UOT91778)	40.4	8.6e-31
MmNV_13	15220	16119	31K (CmNV; UBZ25605)	37.2	3.0e-65
MmNV_14	16237	19365	LEF-8 (ApNV; UOT91780)	54.1	0.0
MmNV_15	19898	21109	P51 (ApNV; UOT91782)	36.4	6.8e-86
MmNV_16	21117	24674	Hypothetical (CmNV; UBZ25608)	36.4	2.7e-124
MmNV_17	24784	25587	–	–	–
MmNV_18	27247	28587	Serine/threonine kinase (CsNV; UVX94888)	33.0	1.8e-17
MmNV_19	28631	30559	ODV-E66 (CsNV; UVX94880)	67.7	0.0
MmNV_20	31101	32339	–	–	–
MmNV_21	32660	34255	PIF-1 (ApNV; UOT91789)	54.3	0.0
MmNV_22	34250	34633	–	–	–
MmNV_23	34623	36845	Hypothetical (CmNV; UBZ25619)	40.3	1.2e-163
MmNV_24	36859	37662	Hypothetical (ApNV; UOT91792)	38.1	1.8e-56
MmNV_25	37812	38579	Hypothetical (ApNV; UOT91793)	28.4	3.5e-23
MmNV_26	38579	39271	PmV-like protein (CmNV; UBZ25622)	41.6	3.3e-60
MmNV_27	39397	40335	Hypothetical (ApNV; UOT91796)	36.1	3.0e-63
MmNV_28	40363	42126	Hypothetical (CsNV; UVX94902)	42.3	4.0e-153
MmNV_29	42094	42405	LEF-5 (predicted)	29.3	4.4e-12
MmNV_30	43095	43397	Putative p6.9	–	–
MmNV_31	43589	44227	Hypothetical (ApNV; UOT91800)	39.4	6.4e-39
MmNV_32	44224	45171	Integrase (HgNV; YP_0100087682)	57.0	6.5e-119
MmNV_33	45288	46487	IAP-3 (MrNV; UHB41752)	27.7	9.0e-09
MmNV_34	46478	47719	LOC108666550-like protein (ApNV; UOT91803)	24.4	2.5e-18
MmNV_35	47835	48320	–	–	–
MmNV_36	48537	49481	–	–	–
MmNV_37	49625	50272	Hypothetical (MrNuV; UHB41753)	42.5	1.4e-50
MmNV_38	50436	51260	–	–	–
MmNV_39	51445	51999	–	–	–
MmNV_40	52358	53248	VLF-1 (CmNV; UBZ25632)	54.7	3.2e-92
MmNV_41	53319	53834	–	–	–
MmNV_42	54463	56121	LEF-9 (ApNV; UOT91809)	56.4	0.0
MmNV_43	56102	57232	38K (CsNV; UVX94914)	46.7	2.3e-51
MmNV_44	57516	58214	Hypothetical (CsNV; UVX94915)	50.6	2.4e-73
MmNV_45	58207	58548	–	–	–
MmNV_46	58582	58887	Hypothetical (ApNV; UOT91813)	38.7	2.9e-16
MmNV_47	58944	59252	–	–	–
MmNV_48	59834	60715	Hypothetical (ApNV; UOT91816)	40.2	1.2e-54
MmNV_49	60701	61393	Hypothetical (PmNV; YP_009051905)	29.6	2.7e-15
MmNV_50	61495	62046	Hypothetical (HgNV; YP_010087698)	35.5	1.8e-32
MmNV_51	62062	63054	Hypothetical (ApNV; UOT91819)	39.1	2.5e-66
MmNV_52	63017	63637	Hypothetical (CmNV; UBZ25652)	41.6	6.9e-49
MmNV_53	63693	65738	PIF-0 (CmNV; UBZ25654)	60.1	0.0
MmNV_54	65788	66558	–	–	–
MmNV_55	66610	67278	Hypothetical (HgNV; YP_010087705)	28	6.8e-13
MmNV_56	67349	69058	Helicase 2 (CsNV; UVX94928)	50	0.0
MmNV_57	69096	69902	–	–	–
MmNV_58	69908	70549	Hypothetical (ApNV; UOT91827)	41.6	1.1e-46
MmNV_59	70539	72470	Helicase 2 (ApNV; UOT91828)	40.2	7.4e-143
MmNV_60	72443	75298	Hypothetical (CsNV; UVX94932)	22.7	2.3e-17
MmNV_61	75307	76167	Hypothetical (ApNV; UOT91830)	39.7	3.5e-58
MmNV_62	76160	76651	Hypothetical (ApNV; UOT91831)	37.4	2.5e-22
MmNV_63	76662	78221	–	23.3	1.6e-15
MmNV_64	78215	78610	Hypothetical (HgNV: YP_010087715)	36.9	4.0e-32
MmNV_65	78666	79082	Ac81 (CsNV; UVX94937)	65.2	1.2e-58
MmNV_66	79079	81259	Hypothetical (ApNV; UOT91837)	35.2	6.1e-53
MmNV_67	81222	81656	PIF-6 (ApNV; UOT91838)	50.0	3.2e-42
MmNV_68	81663	82961	Hypothetical (CsNV; UVX94940)	31.0	7.5e-56
MmNV_69	83077	83832	VLF-1 (ApNV; UOT91840)	37.2	2.7e-48
MmNV_70	83822	85051	LEF-4 (ApNV; UOT91841)	47.6	3.0e-112
MmNV_71	85202	85567	Hypothetical (CmNV; UBZ25672)	33.0	8.6e-20
MmNV_72	85567	86166	PIF-3 (ApNV; UOT91843)	52.6	2.4e-73
MmNV_73	86159	89983	Helicase (CsNV; UVX94945)	52.9	0.0
MmNV_74	89985	90686	PIF-4 (CsNV; UVX94946)	58.6	7.0e-67
MmNV_75	90661	91386	Hypothetical (HgNV; YP_01008772)	37.7	1.8e-48
MmNV_76	91391	92248	Esterase (ApNV; UOT91847)	52.2	3.9e-84
MmNV_77	92249	93448	GbNV_gp67-like (HgNV; YP_010087728)	41.8	4.5e-42
MmNV_78	93944	94282	11K (CmNV; UBZ25680)	38.9	1.5e-16
MmNV_79	94281	95093	Hypothetical (CmNV; UBZ25681)	36.0	2.5e-44

(*continued on next page*)

Table 1 (*continued*)

Gene	Start	Stop	Protein hit (species; accession)	Similarity (%)	e-value
MmNV_80	95135	96265	Apoptosis inhibitor (ApNV; UOT91851)	25.4	6.7e-27
MmNV_81	96235	96924	–	–	–
MmNV_82	97347	97724	–	–	–
MmNV_83	97758	98549	Hypothetical (HgNV; YP_010087736)	45.5	3.3e-75
MmNV_84	98897	99334	Hypothetical (ApNV; UOT91856)	35.5	8.9e-23

MmNV grouped within the *Gammanudivirus* genus based on a 17 gene maximum-likelihood concatenated phylogeny, branching alongside ApNV at a branch distance of 1.095 units with 100% bootstrap support (Fig. 5). The previously suggested unofficial subfamily Betanudivirinae (*Gammanudivirus*, unofficial Epsilonnudivirus, and *Deltanudivirus*) are all well supported on the phylogeny; however, the *Betanudivirus* (HzNV2) branch had lower node support (82%) as did the branch including Penaeus monodon nudivirus (PmNV; from the species *Gammanudivirus pemonodonis*) (66%) (Fig. 5).

3.3. Traits among Nudiviridae and their hosts

Complete genomes of nudiviruses have been sequenced from crustacean and insect hosts that thrive in freshwater, marine, intertidal, and terrestrial environments, or a combination thereof (Fig. 6). Comparison of the genome sizes and predicted protein coding gene number among those identified to date places the new MmNV as the second smallest virus sequenced to date, behind Gryllus bimaculatus nudivirus (GbNV; belonging to the species *Alphanudivirus grybimaculati*) (96,944 bp), but currently as the smallest genomic member of the *Gammanudivirus* genus and encoding the least number of predicted protein coding genes (n = 84) of any nudivirus sequenced to date (Fig. 6).

The terrestrial nudiviruses are the most variable in terms of genome size, taxonomic diversity, and number of protein coding genes (Fig. 6). *Deltanudivirus tipoleraceae* (Tipula oleracea nudivirus; ToNV) (*Deltanudivirus*), *Betanudivirus hezeae* (Helicoverpa zea nudivirus; HzNV2) (*Betanudivirus*), and all *Alphanudivirus* sp., are viral species from terrestrial origins. The *Gammanudivirus* and unofficial Epsilonnudivirus genera consist of a mix of freshwater and marine species with some, such as CmNV and ApNV, infecting hosts with complex lifecycles, such as the intertidal coastline consisting of complex mangrove or rocky shore ecosystems, that span terrestrial and aquatic habitats (Fig. 6). Other nudiviruses infect hosts that are purely aquatic, such as the marine *Homarus gammarus* and riverine *Macrobrachium rosenbergii*. Genome size, number of protein coding genes, or nudivirus genus do not appear to correlate with environment; however, the *Gammanudivirus* and unofficial Epsilonnudivirus genera are only present in Crustacea (all of which are at least semi-aquatic), whereas the other genera infect insects (majority solely terrestrial).

4. Discussion

The first virus from the Florida stone crab, *M. mercenaria*, is

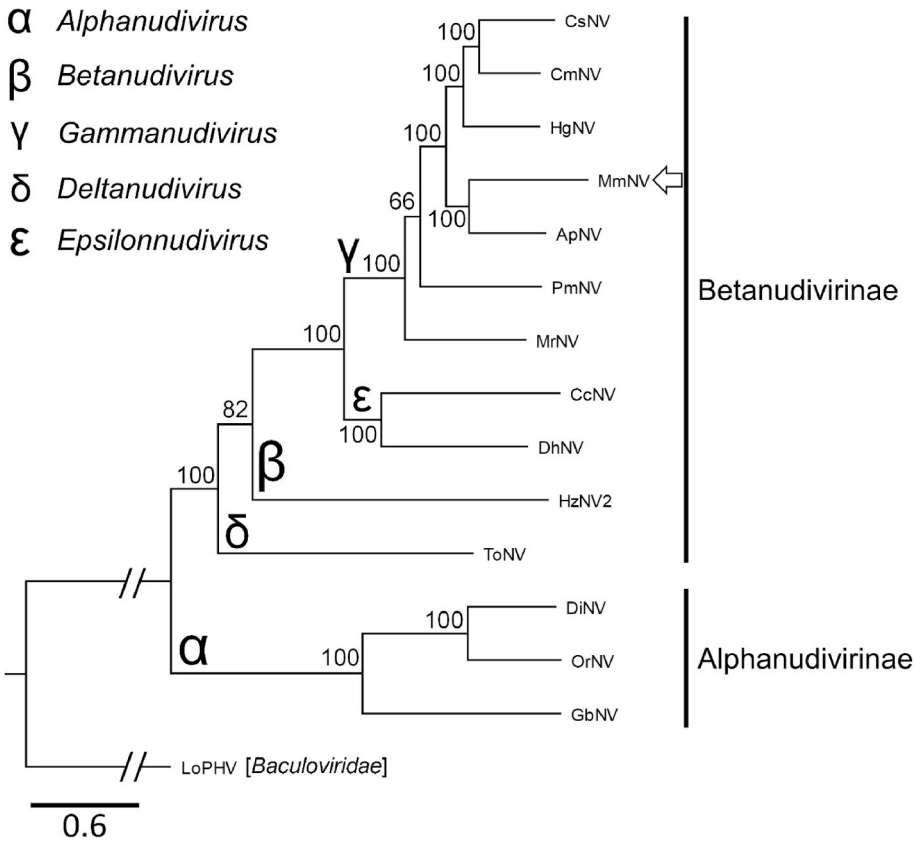

Fig. 5. A maximum-likelihood multi-gene phylogenetic tree including 14 *Nudiviridae* members and 1 *Baculoviridae* outgroup (LoPHV). The two unofficial viral subfamilies Alphanudivirinae and Betanudivirinae are noted next to the tree. The genus is noted on the tree using Greek letters (α, β, γ, δ, ε), that represent the genera as noted in the available key. All bootstrap values are noted on the nodes of the tree and a scale bar is provided (0.6). The new nudivirus, Menippe mercenaria nudivirus (MmNV) is noted on the tree using an arrow. The other nudiviruses are abbreviated as follows, from top to bottom: 'Callinectes sapidus nudivirus' (CsNV), Carcinus maenas nudivirus (CmNV), Homarus Gammarus nudivirus (HgNV), 'Aratus pisonii nudivirus' (ApNV), Penaeus monodon nudivirus (PmNV), 'Macrobrachium rosenbergii nudivirus' (MrNV), Crangon crangon nuivirus (CcNV), 'Dikerogammarus haemobaphes nudivirus' (DhNV), Helicoverpa zea nudivirus 2 (HzNV2), Tipula oleracea nudivirus (ToNV), Drosophlia innubula nudivirus (DiNV), Oryctes rhinoceros nudivirus (OrNV), Gryllus bimaculatus nudivirus (GbNV).

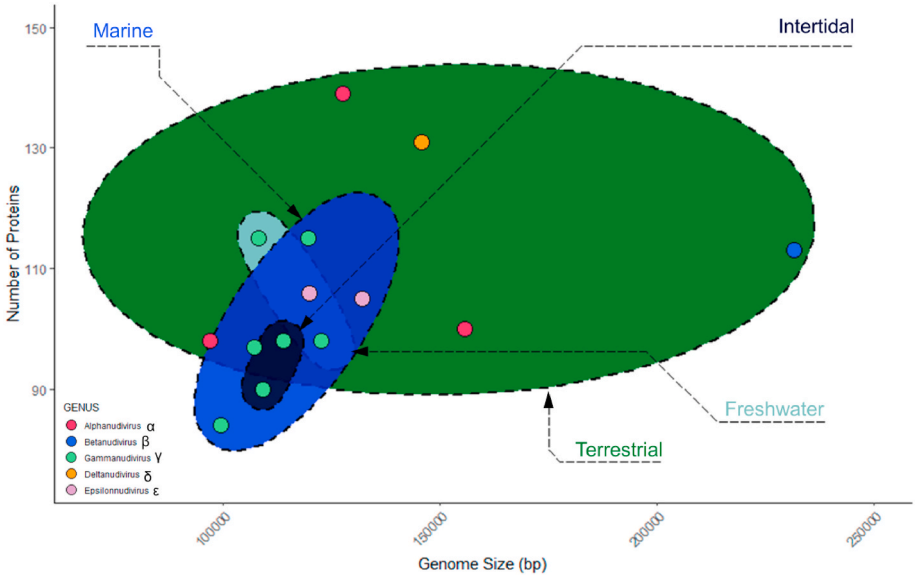

Fig. 6. A comparison between nudivirus taxa (see key), their genome size (x axis), and their predicted protein coding gene count (y axis). The environmental origins of the viruses are used to cluster different groups within ellipsoids (marine, intertidal, freshwater, and terrestrial). Ellipsoids are labelled with their environment, using the same colour as the ellipsoid for the text.

described and assigned to the *Nudiviridae* (Betanudivirinae; *Gammanudivirus*), pending formal recognition by the International Committee for the Taxonomy of Viruses (ICTV). The genome of this new virus is the smallest among the gammanudiviruses, and it equally encodes the smallest number of predicted genes. The virus appears to be restricted to the hepatopancreas of the host, as is common among the *Nudiviridae*. Its discovery provides additional taxonomic insight for the growing *Nudiviridae*, but also brings into question the possible impact it may have on the Florida stone crab fishery.

4.1. Nudiviruses in fished and aquacultured species

The first crustacean nudivirus to have its genome sequenced was PmNV (initially reported in Taiwan), isolated from the hepatopancreas of the black tiger shrimp, *P. monodon*, a readily cultured penaeid shrimp across the Indo-Pacific (Lightner and Redman, 1981; Yang et al., 2014; Marín-Riffo et al., 2021). In aquaculture, the disease is termed "spherical baculovirosis" and can cause mortality in larval and postlarval shrimp; however, growth suppression is often noted in adults (Yang et al., 2014). Other penaeids are resistant to PmNV, suggesting that the virus is an issue mainly contained to *P. monodon* production (Gangnonngiw and Kanthong, 2019). The presence of this virus, among others, eventually resulted in the use of *Penaeus vannamei* in aquaculture over *P. monodon* (Flegel, 2009).

Secondly, during routine histological surveillance of juvenile *H. gammarus* cage-cultured offshore in the UK, HgNV was isolated, sequenced and identified (Holt et al., 2019). This was the second nudivirus formally identified and another example of a culture-based system involving a nudivirus. Although the virus was associated with hepatopancreatic pathology, the infected specimens were not noted with reduced growth or mortality. However, there was a correlation made between a shift in the diversity of the gut microbiome and HgNV infection (Holt et al., 2020), suggesting that the presence of these viruses may change the gut environment of the crustacean host.

A nudivirus in the river prawn, *M. rosenbergii* (GenBank accession: MW484891), which supports a growing fishery (Ofori-Darkwah et al., 2020); one from the shrimp *Crangon crangon* fished in Europe (Verschueren et al., 2019); and a nudivirus from the blue crab *C. sapidus*, which is fished across its range and also used in softshell aquaculture (Bojko et al., 2022b), are all associated with lucrative fished/cultured crustaceans. Although artisanal, there is also a small fishery associated with *Carcinus maenas* in Canada, where CmNV was identified (Bojko et al., 2018; Bateman et al., 2021). Finally, the newly recognised nudivirus from *M. mercenaria*, MmNV, makes the seventh nudivirus associated with an economically important crustacean host, with the remaining *Gammanudivirus* (and unofficial Epsilonnudivirus) diversity present in wild crustaceans of primarily ecological importance (Allain et al., 2020; Bojko et al., 2022a).

Given the common association between nudiviruses and fished species, it is important to explore further diversity of this viral group and critical to determine their effect on fishery dynamics. Disease surveillance is recognised as a vital component of fisheries management, helping to mitigate epizootic impacts and inform upon the conservation and protection of affected species (Groner et al., 2016; Behringer et al., 2020). In the case of *M. mercenaria*, a possible impact of MmNV on stone crab fishery could be reduced growth and juvenile mortality as observed with *P. monodon* populations suffering from PmNV (Yang et al., 2014). Given the rather unconventional fishery method (de-clawing) used to harvest *M. mercenaria*, there is also an opportunity to better understand how different fishing practices may alter nudivirus transmission and pathology.

4.2. Diversity and evolutionary patterns among the nudiviruses

Understanding the evolutionary trajectory of viruses can be important for further exploration of their risk and predictive epidemiology (Albery et al., 2021). In the case of the *Nudiviridae*, their evolution has been explored primarily through phylogenomic analyses, resulting in the current architecture of the *Nudiviridae* family and unofficial Alphanudivirinae and Betanudivirinae subfamilies (Bateman et al., 2021). However, any associated evolutionary mechanisms are yet to be explored experimentally.

Our phylogenetic comparison supports the presence of the *Alphanudivirus*, *Betanudivirus*, *Gammanudivirus*, *Deltranudivirus* and unofficial Epsilonnudivirus genera to date, as well as the unofficial sub-family partition. However, our comparison of genome size, protein coding gene number and environment suggest that neither genome size nor gene number correlate with certain environments, especially in the terrestrial viruses, where some alphanudiviruses have small genomes in comparison to the larger *Betanudivirus* (Fig. 6). There is a distinct

difference between insect-infecting and crustacean-infecting nudiviruses, which corroborates with previous studies, but looking in finer detail at the Crustacea reveals that there are some odd phylogenetic relationships between infected Decapod taxa and their nudiviruses.

More closely related decapods do not necessarily have more related nudiviruses. In our phylogeny, HgNV (lobster host) branches in the middle of several crab-infecting species. The two shrimp infecting viruses remain on separate branches. Finally, Crangon crangon nudivrius (CcNV; from the species *Gammanudivirus cracrangonis*) (from a decapod shrimp) groups more closely with DhNV, a nudivirus from an amphipod (Peracarida). Although there is a clear phylogenomic distinction between insect-infecting and crustacean-infecting viral taxa, the viruses do not follow the evolutionary similarity of their hosts within the Crustacea (Fig. 5).

Finally, a geographic comparison of the available viruses suggests that hosts from the same area may have more related viruses. ApNV and MmNV form their own branch and share a reasonable level of gene synteny, as well as being from Florida. However, an exception to this rule is CsNV, which infects *C. sapidus* also from Florida but is more related to CmNV, which infects *C. maenas* from Europe (Bojko et al., 2022b). However, *C. maenas* is invasive in the USA while *C. sapidus* is invasive in Europe. Greater taxonomic diversity and exploration of further viral traits is necessary to explore different avenues of evolution in this group.

4.3. Conclusions

Our perception of *Nudiviridae* diversity continues to expand through further application of genomic and pathological tools (Bojko et al., 2022b). It is evident that the majority of gammanudiviruses discovered to date are from economically important species, totalling seven potential pathogenic risks to crustaceans that support artisanal fisheries, industrial fisheries, or aquaculture. Our comparison between viral traits and host environment does not explain the diversity we currently see, suggesting that viral evolution, and potentially host-switching events among the Decapoda, may better explain viral relatedness and virus-host relationships.

Our new discovery of MmNV marks the first virus identified from the Florida stone crab and has the smallest genome of a *Gammanudivirus* identified to date. The presence of this virus should promote research into the effects of this viral group on an unconventional fishing system, where claw removal and the return of injured animals to the sea could alter the pathological dynamic of this virus's transmission and prevalence.

CRediT authorship contribution statement

Jamie Bojko: Conceptualization, histology, genomics, plotting, writing. **Elizabeth Duermit-Moreau:** Conceptualization, transmission electron microscopy, sample collection, writing, Funding acquisition. **Ryan Gandy:** Conceptualization, sample collection. **Donald C. Behringer:** Conceptualization, writing, Supervision, Funding acquisition.

Declaration of competing interest

The authors declare that they have no known competing financial interests or personal relationships that could have appeared to influence the work reported in this paper.

Acknowledgements

We would like to thank all those who helped with field collection and necropsy including T. Allain, E. An, C. Branam, J. Harrington, H. Powless, K. Rose, A. Scro, N. Stephens, C. Stratton, E. Walters. Thank you to the FWC-FWRI Histology Department for processing histology cassettes into H&E-stained slides. EDM was supported by a Pre-eminent Alumni Fellowship from the University of Florida College of Agriculture and Life Sciences. This research was funded by Florida Sea Grant Aylesworth and Guy Harvey Scholarships, and the Cynthia Melnick Endowment.

References

Albery, G.F., Becker, D.J., Brierley, L., Brook, C.E., Christofferson, R.C., Cohen, L.E., et al., 2021. The science of the host–virus network. Nature microbiology 6 (12), 1483–1492.

Allain, T.W., Stentiford, G.D., Bass, D., Behringer, D.C., Bojko, J., 2020. A novel nudivirus infecting the invasive demon shrimp *Dikerogammarus haemobaphes* (Amphipoda). Sci. Rep. 10 (1), 1–13.

Bankevich, A., Nurk, S., Antipov, D., Gurevich, A.A., Dvorkin, M., Kulikov, A.S., et al., 2012. SPAdes: a new genome assembly algorithm and its applications to single-cell sequencing. J. Comput. Biol. 19 (5), 455–477.

Bateman, K.S., Kerr, R., Stentiford, G.D., Bean, T.P., Hooper, C., Van Eynde, B., et al., 2021. Identification and full characterisation of two novel crustacean infecting members of the family *Nudiviridae* provides support for two subfamilies. Viruses 13 (9), 1694.

Behringer, D.C., Butler, M.J.I.V., Shields, J.D., Moss, J., 2012. PaV1 infection in the Florida spiny lobster fishery and its effects on trap function and disease transmission. Can. J. Fish. Aquat. Sci. 69, 136–144.

Behringer, D.C., Wood, C.L., Krkosek, M., Bushek, D., 2020. Chapter 10: disease in fisheries and aquaculture. In: Behringer, D.C., Silliman, B.R., Lafferty, K.D. (Eds.), Marine Disease Ecology. Oxford University Press, Oxford, UK.

Besemer, J., Lomsadze, A., Borodovsky, M., 2001. GeneMarkS: a self-training method for prediction of gene starts in microbial genomes. Implications for finding sequence motifs in regulatory regions. Nucleic Acids Res. 29 (12), 2607–2618.

Bojko, J., Stebbing, P.D., Dunn, A.M., Bateman, K.S., Clark, F., Kerr, R.C., et al., 2018. Green crab *Carcinus maenas* symbiont profiles along a North Atlantic invasion route. Dis. Aquat. Org. 128 (2), 147–168.

Bojko, J., Burgess, A.L., Allain, T.W., Ross, E.P., Pharo, D., Kreuze, J.F., Behringer, D.C., 2022a. Pathology and genetic connectedness of the mangrove crab (*Aratus pisonii*)–a foundation for understanding mangrove disease ecology. Animal Diseases 2 (1), 1–16.

Bojko, J., Walters, E., Burgess, A., Behringer, D.C., 2022b. Rediscovering "Baculovirus-A" (Johnson, 1976): the complete genome of 'Callinectes sapidus nudivirus'. J. Invertebr. Pathol. 194, 107822.

Bolger, A.M., Lohse, M., Usadel, B., 2014. Trimmomatic: a flexible trimmer for Illumina sequence data. Bioinformatics 30 (15), 2114–2120.

Duermit, E., Kingsley-Smith, P.R., Wilber, D.H., 2015. The consequences of claw removal on stone crabs *Menippe* spp. and the ecological and fishery implications. N. Am. J. Fish. Manag. 35, 895–905.

Duermit, E., Shervette, V., Whitaker, J.D., Kingsley-Smith, P.R., Wilber, D., 2017. A field assessment of claw removal impacts on the movement and survival of stone crabs *Menippe* spp. Fish. Res. 193, 43–50.

Duermit-Moreau, E., Bojko, J., Behringer, D.C., 2022. Cyanobacterial blooms alter benthic community structure and parasite prevalence among invertebrates in Florida Bay, USA. Mar. Ecol. Prog. Ser. 694, 29–44.

Flegel, T.W., 2009. Current status of viral diseases in Asian shrimp aquaculture. The Israeli Journal of Aquaculture 229–239.

Freeman, D.J., MacDiarmid, A.B., 2009. Healthier lobsters in a marine reserve: effects of fishing on disease incidence in the spiny lobster, *Jasus edwardsii*. Mar. Freshw. Res. 60, 140–145.

Gandy, R., Crowley, C., Chagaris, D., Crawford, C., 2016. The effect of temperature on release mortality of declawed *Menippe mercenaria* in the Florida stone crab fishery. Bull. Mar. Sci. 92, 1–15.

Gangnonngiw, W., Kanthong, N., 2019. Evidence that the whiteleg shrimp *Penaeus* (*Litopenaeus*) *vannamei* is refractory to infection by Penaeus monodon nudivirus (PmNV), also known as MBV. Aquaculture 499, 290–294.

Gasteiger, E., Gattiker, A., Hoogland, C., Ivanyi, I., Appel, R.D., Bairoch, A., 2003. ExPASy: the proteomics server for in-depth protein knowledge and analysis. Nucleic Acids Res. 31, 3784–3788.

Groner, M.L., Maynard, J., Breyta, R., Carnegie, R.B., Dobson, A., Friedman, C.S., et al., 2016. Managing marine disease emergencies in an era of rapid change. Phil. Trans. Biol. Sci. 371 (1689), 20150364.

Gurevich, A., Saveliev, V., Vyahhi, N., Tesler, G., 2013. QUAST: quality assessment tool for genome assemblies. Bioinformatics 29 (8), 1072–1075.

Hancock, E.R., Griffen, B.D., 2017. The energetic consequences of temperature variation and sequential autotomization for the stone crab, *Menippe* spp. Marine Ecolology Progress Series 582, 133–146.

Holt, C.C., Stone, M., Bass, D., Bateman, K.S., van Aerle, R., Daniels, C.L., et al., 2019. The first clawed lobster virus Homarus gammarus nudivirus (HgNV n. sp.) expands the diversity of the *Nudiviridae*. Sci. Rep. 9 (1), 1–15.

Holt, C.C., van der Giezen, M., Daniels, C.L., Stentiford, G.D., Bass, D., 2020. Spatial and temporal axes impact ecology of the gut microbiome in juvenile European lobster (*Homarus gammarus*). ISME J. 14 (2), 531–543.

Humes, A.G., 1941. Notes on *Octolasmis müilleri* (Coker), a barnacle commensal on crabs. Trans. Am. Microsc. Soc. 60, 101–103.

Lightner, D.V., Redman, R.M., 1981. A baculovirus-caused disease of the penaeid shrimp, *Penaeus monodon*. J. Invertebr. Pathol. 38 (2), 299–302.

Marín-Riffo, M.C., Raadsma, H.W., Jerry, D.R., Coman, G.J., Khatkar, M.S., 2021. Bioeconomic modelling of hatchery, grow-out and combined business of Australian black tiger shrimp Penaeus monodon farming. Rev. Aquacult. 13 (3), 1695–1708.

Muller, R.G., Bert, T.M., Gerhart, S.D., 2006. The 2006 stock assessment update for the stone crab, *Menippe* spp., fishery in Florida. Florida Fish and Wildlife Conservation Commission. IHR 11, 47.

Nguyen, L.T., Schmidt, H.A., Von Haeseler, A., Minh, B.Q., 2015. IQ-TREE: a fast and effective stochastic algorithm for estimating maximum-likelihood phylogenies. Mol. Biol. Evol. 32 (1), 268–274.

Ofori-Darkwah, P., Adjei-Boateng, D., Edziyie, R.E., 2020. The status of *Macrobrachium* fishery and its market in southern Ghana. Journal of Fisheries and Coastal Management 2, 65–74.

R Core Team, 2013. R: A Language and Environment for Statistical Computing.

Santos, C., Norenburg, J.L., Bueno, S.L., 2006. Three new species of *Carcinonemertes* (Nemertea, Carcinonemertidae) from the southeastern coast of Brazil. J. Nat. Hist. 40 (15–16), 915–930.

Sheppard, M., Walker, A., Frischer, M.E., Lee, R.F., 2003. Histopathology and prevalence of the parasitic dinoflagellate, *Hematodinium* sp, in crabs (*Callinectes sapidus, Callinectes similis, Neopanope sayi, Libinia emarginata, Menippe mercenaria*) from a Georgia estuary. J. Shellfish Res. 22 (3), 873–880.

Sprague, V., 1949. Species of *Nematopsis* in *Ostrea virginica*. J. Parasitol. 35, 243–256.

Sprague, V., Orr, P.E., 1955. *Nematopsis ostrearum* and *N. prytherchi* (Eugregarinina: porosporidae) with special reference to the host-parasite relations. J. Parasitol. 41 (1), 89–104.

Stratton, C.E., Reisinger, L.S., Behringer, D.C., Reinke, A.W., Bojko, J., 2023a. *Alternosema astaquatica* n. sp. (Microsporidia: enterocytozoonida), a systemic parasite of the crayfish *Faxonius virilis*. J. Invertebr. Pathol., 107948

Stratton, C.E., Kabalan, B.A., Bolds, S.A., Reisinger, L.S., Behringer, D.C., Bojko, J., 2023b. *Cambaraspora faxoni* n. sp. (Microsporidia: glugeida) from native and invasive crayfish in the USA and a novel host of *Cambaraspora floridanus*. J. Invertebr. Pathol., 107949

Verschueren, B., Lenoir, H., Soetaert, M., Polet, H., 2019. Revealing the by-catch reducing potential of pulse trawls in the brown shrimp (*Crangon crangon*) fishery. Fish. Res. 211, 191–203.

Wickham, H., 2011. ggplot2. Wiley interdisciplinary reviews: Comput. Stat. 3 (2), 180–185.

Wood, C.L., Sandin, S.A., Zgliczynski, B., Guerra, A.S., Micheli, F., 2014. Fishing drives declines in fish parasite diversity and has variable effects on parasite abundance. Ecology 95 (7), 1929–1946.

Yang, Y.T., Lee, D.Y., Wang, Y., Hu, J.M., Li, W.H., Leu, J.H., et al., 2014. The genome and occlusion bodies of marine Penaeus monodon nudivirus (PmNV, also known as MBV and PemoNPV) suggest that it should be assigned to a new nudivirus genus that is distinct from the terrestrial nudiviruses. BMC Genom. 15 (1), 1–24.